Study of Some Elastic Properties for Sandwich Beams Reinforced with Different Types of Fabric

DUMITRU BOLCU[1]*, MARIUS MARINEL STANESCU[2], ION CIUCA[3], SONIA DEGERATU[4], MARIUS-ALEXANDRU GROZEA[5]

[1] University of Craiova, Department of Mechanics, 165 Calea Bucureşti, 200620, Craiova, Romania

[2] University of Craiova, Department of Applied Mathematics,13 A.I. Cuza, 200396, Craiova, Romania

[3] Politehnica University of Bucharest,Department of Materials Science and Engineering, 313 Splaiul Independentei, 060042, Bucharest, Romania

[4] University of Craiova,, Faculty for Engineering in Electromechanics, Environment and Industrial IT, Craiova, Romania.

[5] Politehnica University of Bucharest, Strength of Materials Department, 313 Splaiul Independentei, 060042, Bucharest, Romania

In this paper, we determined a state of stress, which verifies the Cauchy equations of equilibrium, the conditions of continuity on the surfaces between layers and boundary conditions for a sandwich beam subjected to tensile test. We customized the relations, previously obtained, for a composite beam consisting of two layers. Using a mediation formula for strain and stress, we obtained a new formula for the calculus of the longitudinal modulus of elasticity, when the constituent materials have different Poisson ratios. Considering the maximum stress reached in the layers, we determined a formula, which helps us to determine the order in which the two layers will break. We did experimental measurements for test samples made from polyesteric resin, reinforced with fiber glass fabric, carbon and carbon-kevlar.

Keywords: composite materials, characteristic curve, elasticity modulus

The composite plates and beams may be analyzed using many theories that differ mostly by including or neglecting the effects of angular strain and, rotational inertia, respectively. Hashin and Rosen use the classical theory [1], based on the hypothesis that a straight-line, normal on the median surface before deformation, remains straight and normal on the median surface during the deformation too. For laminates with a ratio between the modulus of elasticity E and the shear modulus G reaching values of $25-40$, it be can proven that this theory overestimates the natural frequencies of the structure.

Another theory (First – order Shear Deformation Theory – FSDT) was developed [2] and later modified [3]. This theory relies on a linear distribution of the shear stress and requests a correction factor similar with the one from isotropic plates. This theory states that a straight line normal to median plane before deformation remains straight without keeping the normality on the median surface during deformation.

Exact theories rely on a non-linear distribution of shear stress along the thickness of the plate or beam. The inclusion of high order terms implies the inclusion of supplementary unknowns. Moreover, when fulfilling both the parabolic distribution of shear stress in thickness and the limit conditions on external surfaces, a correction factor is not necessary anymore. Based on this fact, it was developed a theory [4] (High – order Shear Deformation Theory – HSDT) where it is assumed that the stress and strains normal to the median plane are null. Another theory in which the stresses normal to the median plane are considered too, has been developed in [5-6] and removes a series of contradictions appearing in previous theories by accepting non linear factors of shear stress in thickness; they didn't also neglect some of the normal stress obtained by the loading of the composite structure.

In [7] were obtained theoretical results and experimental determinations. Using a matrix method were determined the main elastic characteristics of composite materials and their variation depending on the volumetric proportion of reinforcement.

The studies of the composite materials dynamics reserved a special place for sandwich beams made from several overlapped layers with similar thickness. Most studies refer to three layer sandwich beams, the middle layer having visco-elastic behavior and the inferior and superior layers having extra elastic and resilience properties. Other authors having similar studies on the behavior of these materials suggested the following:

-there is a continuity of displacements and stress between layers;

-there is no deformation along the thickness of the beam;

-the transversal inertial forces are dominant, neglecting longitudinal inertia and rotational inertia of the beam section;

-the external layers have elastic behaviour and are subject to pure bending and the core has elastic or visco-elastic behaviour taking over shear stress;

- the core is not subject to normal stress.

Based on these hypotheses, there have been developed models considered to be the fundamentals of DTMM theory [8-10]. Considering this theory, it was adapted a variation approach, obtained equations for sandwich plates taking also into consideration different angular deformation for the layers and managing to estimate the stress between the layers [11].

The most common types of damage in fibrous composites are fiber breakage, fiber/matrix debonding, matrix cracks, fiber kinking and for large diameter fibers, radial cracks in the fibers. We consider damage that can only increase or remain constant over time; there is no healing.

As damage occurs, the material loses stiffness and exhibits nonlinear, inelastic response with permanent strains after unloading. The inelastic response is the result

* *email: dbolcu@yahoo.com*

of sliding friction at damage sites as well as any inelastic response of the constituent phases. Since the process is irreversible, nonlinear analysis techniques must be employed.

The general damage theory that serves as the foundation for this model was originally proposed [12]. Later the general damage theory was adapted for application to laminated composites [13]. The theory has been proven to be very robust for predicting the damaged response of composites under a wide variety of conditions. It is based upon the method of local state expressed in terms of state variables and the associated thermodynamic forces. According to [14], "the method of local state" postulates that the thermodynamic state of a material medium at a given point and instant is completely defined by the knowledge of the values of a certain number of variables at that instant, which depend only upon the (material) point considered. Since the time derivatives of these variables are not involved in the definition of the state, this hypothesis implies that any evolution can be considered as a succession of equilibrium states [15].

For the most general configuration, Ladeveze's theory considers a composite to be a laminated structure consisting of two elementary constituents: layers of composite and interfaces that separate the composite layers. The interface is considered to be a mechanical surface connecting two adjacent composite layers; it is included in the model only when delamination is of interest. When delamination is not of interest, the model is an assemblage of composite layers.

In composite materials containing fiber or particulate reinforcement the interface separating matrix from inclusion is widely believed to be a dominant influence affecting the overall stiffness and damage tolerance characteristics of the composite. Likewise damage accumulation in a composite often depends on the character of the mechanical response of the interface that, in the case of a weak interface, may precipitate such separation phenomena as brittle or ductile decohesion. In many fiber-reinforced composite systems weak interfaces or desirable since they generally raise the toughness, however, are often at the expense of composite stiffness. Accurate assessment of overall stiffness characteristics of a composite containing fiber weakly bonded to the matrix is therefore extremely important in the attempt to obtain improved composite performance.

Interlaminar stress near free edges of composite beams are mainly responsible for delamination failures. Numerous studies have been undertaken to investigate interlaminar stress and failures of laminated composites [18]. In [16] is studied the interlaminar tensile strength under static and fatigue loads including the temperature and moisture effects. In [17] and [19] is studied the effect of geometric nonlinearities on free-edge stress fields of beams. In [20] is investigated the response and failure for dropped-ply laminates tested in flat-end compression, and [21] have shown that the times for delamination onset occurrences in composites can be predicted probabilistically.

Theoretical Considerations

We consider a composite beam with rectangular section, which has the width *2b* having layers (each of different materials), with constant thickness on the entire beam length. The beam is referenced to a coordinate system, with the axis oriented as follows (fig. 1):

- axis x_1, on longitudinal direction of the beam;
- axis x_2, on width direction of the beam;
- axis x_3, on thickness direction of the beam

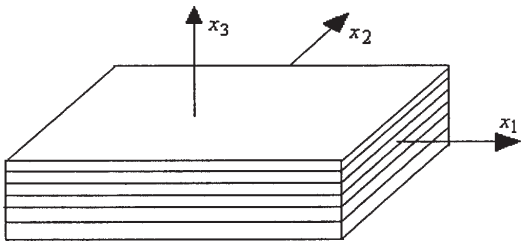

Fig. 1. Coordinate system of the beam

The beam is subject to a tensile test.

Generally, because the materials which the beam layers are made of have different Poisson ratios, then stress state shall be complex. We believe that the stress tensor has all of his components nonzero. If the length of the beam is big (relative to other dimensions), we can accept that in the middle area of the beam, the stress state that arises, does not depend on the coordinate x_1 ($\sigma_{ij}=\sigma_{ij}(x_2, x_3)$). In these situation, the Cauchy equations of equilibrium, have the following aspect:

$$\begin{aligned} &\sigma_{12,2}+\sigma_{13,3}=0,\\ &\sigma_{22,2}+\sigma_{23,3}=0,\\ &\sigma_{32,2}+\sigma_{33,3}=0. \end{aligned} \tag{1}$$

Due to the symmetry, the tangential stresses σ_{12} and σ_{23}, must satisfy the following conditions:

$$\begin{aligned} &\sigma_{12}(-x_2,x_3)=-\sigma_{12}(x_2,x_3),\\ &\sigma_{23}(-x_2,x_3)=-\sigma_{23}(x_2,x_3). \end{aligned} \tag{2}$$

In addition, these tensions must be zero on the lateral surfaces of the beam, namely:

$$\begin{aligned} &\sigma_{12}(-b,x_3)=\sigma_{12}(b,x_3)=0,\\ &\sigma_{23}(-b,x_3)=\sigma_{23}(b,x_3)=0. \end{aligned} \tag{3}$$

With these restrictions, in layer „*i*", the developments in Fourier series (as functions of x_2) for the two tensions are of the form:

$$\begin{aligned} \sigma_{12}^{(i)}&=\sum_{n=1} f_n^{(i)}(x_3)\sin\frac{n\pi x_2}{b},\\ \sigma_{23}^{(i)}&=\sum_{n=1} g_n^{(i)}(x_3)\sin\frac{n\pi x_2}{b}. \end{aligned} \tag{4}$$

From the Cauchy conditions, we conclude that:

$$\begin{aligned} \sigma_{13}^{(i)}&=-\sum_{n=1}\frac{n\pi}{b}F_n^{(i)}(x_3)\cos\frac{n\pi x_2}{b},\\ \sigma_{22}^{(i)}&=\sum_{n=1}\frac{b}{n\pi}\left(g_n^{(i)}\right)'(x_3)\left(\cos\frac{n\pi x_2}{b}-(-1)^n\right),\\ \sigma_{33}^{(i)}&=-\sum_{n=1}\frac{n\pi}{b}G_n^{(i)}(x_3)\cos\frac{n\pi x_2}{b}, \end{aligned} \tag{5}$$

in which $F_n^{(i)}(x_3)$ and $G_n^{(i)}(x_3)$ are primitive for functions $f_n^{(i)}(x_3)$ and $g_n^{(i)}(x_3)$.

These stresses check the symmetry conditions:

$$\begin{aligned} &\sigma_{13}^{(i)}(-x_2,x_3)=\sigma_{13}^{(i)}(x_2,x_3),\\ &\sigma_{22}^{(i)}(-x_2,x_3)=\sigma_{22}^{(i)}(x_2,x_3),\\ &\sigma_{33}^{(i)}(-x_2,x_3)=\sigma_{33}^{(i)}(x_2,x_3), \end{aligned} \tag{6}$$

and on the lateral surface of the beam we have

$$\sigma_{22}^{(i)}(-b,x_3)=\sigma_{22}^{(i)}(b,x_3). \tag{7}$$

Taking the forms of these components (of the stress tensor) into account, it is accepted for the normal stress $\sigma_{11}^{(i)}$ too, the following form:

$$\sigma_{11}^{(i)}(x_2,x_3)=\sum_{n=1}\left[h_n^{(i)}(x_3)\cos\frac{n\pi x_2}{b}+p_n^{(i)}(x_3)\right]. \quad (8)$$

If the materials (of the beam layers) are linear elastic, then the components of strain tensor for the layer „ " shall have the expressions:

$$\begin{aligned}
\varepsilon_{11}^{(i)}&=c_{11}^{(i)}\sum_{n=1}\left[h_n^{(i)}(x_3)\cos\frac{n\pi x_2}{b}+p_n^{(i)}(x_3)\right]+\\
&+c_{12}^{(i)}\sum_{n=1}\frac{b}{n\pi}\left(g_n^{(i)}\right)'(x_3)\left(\cos\frac{n\pi x_2}{b}-(-1)^n\right)-c_{13}^{(i)}\sum_{n=1}\frac{n\pi}{b}G_n^{(i)}(x_3)\cos\frac{n\pi x_2}{b},\\
\varepsilon_{22}^{(i)}&=c_{12}^{(i)}\sum_{n=1}\left[h_n^{(i)}(x_3)\cos\frac{n\pi x_2}{b}+p_n^{(i)}(x_3)\right]+\\
&+c_{22}^{(i)}\sum_{n=1}\frac{b}{n\pi}\left(g_n^{(i)}\right)'(x_3)\left(\cos\frac{n\pi x_2}{b}-(-1)^n\right)-c_{23}^{(i)}\sum_{n=1}\frac{n\pi}{b}G_n^{(i)}(x_3)\cos\frac{n\pi x_2}{b},\\
\varepsilon_{33}^{(i)}&=c_{13}^{(i)}\sum_{n=1}\left[h_n^{(i)}(x_3)\cos\frac{n\pi x_2}{b}+p_n^{(i)}(x_3)\right]+\\
&+c_{23}^{(i)}\sum_{n=1}\frac{b}{n\pi}\left(g_n^{(i)}\right)'(x_3)\left(\cos\frac{n\pi x_2}{b}-(-1)^n\right)-c_{33}^{(i)}\sum_{n=1}\frac{n\pi}{b}G_n^{(i)}(x_3)\cos\frac{n\pi x_2}{b},\\
\varepsilon_{23}^{(i)}&=c_{44}^{(i)}\sum_{n=1}g_n^{(i)}(x_3)\sin\frac{n\pi x_2}{b},\\
\varepsilon_{13}^{(i)}&=-c_{55}^{(i)}\sum_{n=1}\frac{n\pi}{b}F_n^{(i)}(x_3)\cos\frac{n\pi x_2}{b},\\
\varepsilon_{12}^{(i)}&=c_{66}^{(i)}\sum_{n=1}f_n^{(i)}(x_3)\sin\frac{n\pi x_2}{b},
\end{aligned} \quad (9)$$

where $c_{11}^{(i)}$, $c_{12}^{(i)}$, $c_{13}^{(i)}$, $c_{22}^{(i)}$, $c_{23}^{(i)}$, $c_{33}^{(i)}$, $c_{44}^{(i)}$, $c_{55}^{(i)}$, $c_{66}^{(i)}$ are elastic coefficients for the material of the „ " layer.

Restrictions that must be satisfied by the functions $f_n^{(i)}$, $g_n^{(i)}$, $h_n^{(i)}$, $p_n^{(i)}$ are determined from continuity conditions for the σ_{13}, σ_{23}, σ_{33} stresses and the ε_{11}, ε_{22}, ε_{12} strain, which exist on the separation surfaces between layers. In addition, the stresses σ_{13}, σ_{23}, σ_{33} must be canceled on upper and lower surfaces of the beam.

After fulfilling of all these restrictions, in beam section, we can determine

-medium stress:

$$\overline{\sigma}_{11}=\frac{1}{S}\iint_{(S)}\sigma_{11}dS \quad (10)$$

-medium strain:

$$\overline{\varepsilon}_{11}=\frac{1}{S}\iint_{(S)}\varepsilon_{11}dS \quad (11)$$

Thus, we can calculate the longitudinal modulus of elasticity for the beam, with the relation:

$$E_L=\frac{\overline{\sigma}_{11}}{\overline{\varepsilon}_{11}}. \quad (12)$$

With (8), we determine the maximum stress in each layer. The fracture of the beam phenomenon, begins when the stress state in a layer reaches the fracture limit of the material of that layer. After this moment, increases of the stress appear in the others layers too.

If the beam is made from two layers, we choose the coordinate system with axis x_1 and x_2, in the separation plane between those two layers. Denote with (1) , the layer of material placed below the separation surface, and with (2) , the layer of material placed above the separation surface. We consider that the thickness of material (1) is α, and the thickness of material (2) is β. If the two materials, have different Poisson ratios, then the continuity conditions are satisfied if the functions (previously defined) have the expressions:

$$\begin{aligned}
G_n^{(1)}(x_3)&=\frac{A_n}{\alpha^2}(x_3+\alpha)^3-\frac{A_n}{\alpha}(x_3+\alpha)^2,\\
G_n^{(2)}(x_3)&=\frac{A_n}{\beta^2}(x_3-\beta)^3-\frac{A_n}{\beta}(x_3-\beta)^2,\\
p_n^{(1)}(x_3)&=\frac{(-1)^n b}{n\pi(\upsilon_2-\upsilon_1)}\left[(1-\upsilon_1\upsilon_2)\left(g_n^{(1)}\right)'(x_3)-\frac{E_1}{E_2}\left(1-\upsilon_2^2\right)\left(g_n^{(2)}\right)'(x_3)\right],\\
p_n^{(2)}(x_3)&=\frac{(-1)^n b}{n\pi(\upsilon_2-\upsilon_1)}\left[\frac{E_2}{E_1}\left(1-\upsilon_1^2\right)\left(g_n^{(1)}\right)'(x_3)-(1-\upsilon_1\upsilon_2)\left(g_n^{(2)}\right)'(x_3)\right],\\
h_n^{(1)}(x_3)&=\frac{1}{\upsilon_2-\upsilon_1}\left[-\frac{n\pi}{b}\upsilon_1(1+\upsilon_2)G_n^{(1)}(x_3)+\frac{n\pi}{b}\frac{E_1}{E_2}\upsilon_2(1+\upsilon_2)G_n^{(2)}(x_3)-\right.\\
&\left.-\frac{b}{n\pi}(1-\upsilon_1\upsilon_2)\left(g_n^{(1)}\right)'(x_3)+\frac{b}{n\pi}\frac{E_1}{E_2}\left(1-\upsilon_2^2\right)\left(g_n^{(2)}\right)'(x_3)\right]\\
h_n^{(2)}(x_3)&=\frac{1}{\upsilon_2-\upsilon_1}\left[-\frac{n\pi}{b}\frac{E_2}{E_1}\upsilon_1(1+\upsilon_1)G_n^{(1)}(x_3)+\frac{n\pi}{b}\upsilon_2(1+\upsilon_1)G_n^{(2)}(x_3)-\right.\\
&\left.-\frac{b}{n\pi}\frac{E_2}{E_1}\left(1-\upsilon_1^2\right)\left(g_n^{(1)}\right)'(x_3)+\frac{b}{n\pi}(1-\upsilon_1\upsilon_2)\left(g_n^{(2)}\right)'(x_3)\right].
\end{aligned} \quad (13)$$

In these conditions, the longitudinal modulus of elasticity calculated with (12), is:

$$E_L=\frac{E_1^2V_1^2\left(1-\upsilon_2^2\right)(3+V_2)+E_2^2V_2^2\left(1-\upsilon_1^2\right)(3+V_1)}{E_1V_1\left(1-\upsilon_2^2\right)(3+V_2)+E_2V_2\left(1-\upsilon_1^2\right)(3+V_1)}+$$
$$+\frac{E_1E_2V_1V_2[(1-\upsilon_2)(1+\upsilon_1)(3+V_1)+(1-\upsilon_1)(1+\upsilon_2)(3+V_2)]}{E_1V_1\left(1-\upsilon_2^2\right)(3+V_2)+E_2V_2\left(1-\upsilon_1^2\right)(3+V_1)}, \quad (14)$$

where:

- ν_1 and ν_2 are the Poisson ratios for the two layers;
- V_1 and V_2 are volumetric proportions of the two materials.

The relation may apply even if the Poisson ratios are equal (namely $\nu_1=\nu_2$), so that we have:

$$E_L=E_1V_1+E_2V_2, \quad (15)$$

which is the classical relation for the calculus of the elasticity modulus.

The graphical representation of the elasticity modulus E_L for a composite made of polyesteric resin reinforced with fiber glass fabric, according to the volumetric proportion of the reinforcement V, calculated with (14), is given in figure 2.

In figure 2 we can see that the variation of longitudinal modulus of elasticity is almost proportional to the volumetric proportion of the materials.

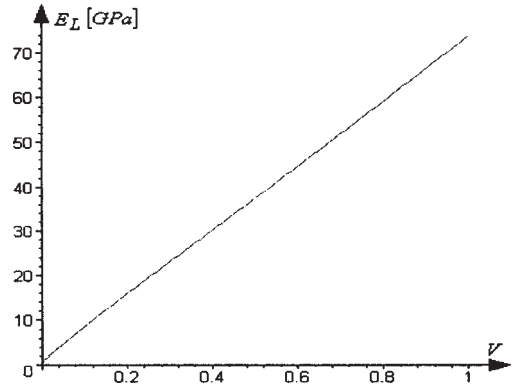

Fig. 2. Variation of E_L with volumetric proportion

The graphical representation of the ratio between the elasticity modulus E_L (for a composite material) and elasticity modulus E_1, according to the volumetric proportion of the reinforcement V and the ratio $x=E_2/E_1$, for $\nu_1=0.25$ and $\nu_2=0.4$, is given in figure 3.

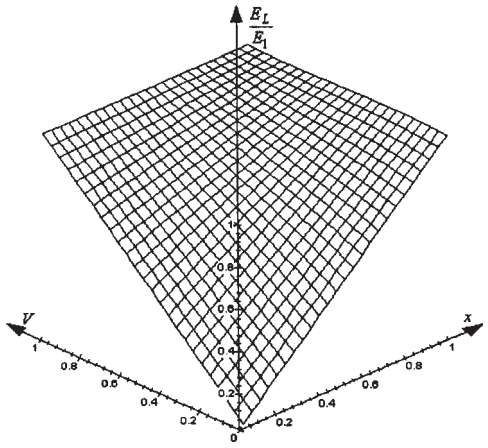

Fig. 3 E_L/E_1 as function of the volumetric proportion V and the E_2/E_1 ratio

Comparing the maximum stress in the two layers, we state that the following expression is important:

$$e=\frac{E_2\sigma_{r_1}\left[E_1V_1(1-\upsilon_1\upsilon_2)+E_2V_2\left(1-\upsilon_1^2\right)\right]}{E_1\sigma_{r_2}\left[E_2V_2(1-\upsilon_1\upsilon_2)+E_1V_1\left(1-\upsilon_2^2\right)\right]}, \qquad (16)$$

where σ_{r1} and σ_{r2} are the fracture limits for the materials of the two layers.

If $e<1$, then the fracture arises in layer (1), and the load will be taken by layer (2), and the damage of the test sample occurs when the layer (2) is broken. If $e>1$, then the fracture begins with the layer (2), the damage of the test sample occurs at the fracture of layer (1).

The graphical representation of *e* (for a ratio $\sigma_{r1}/\sigma_{r2}=30$) according to the volumetric proportion V and ratio of the elasticity modules $x=E_2/E_1$, is given in figure 4.

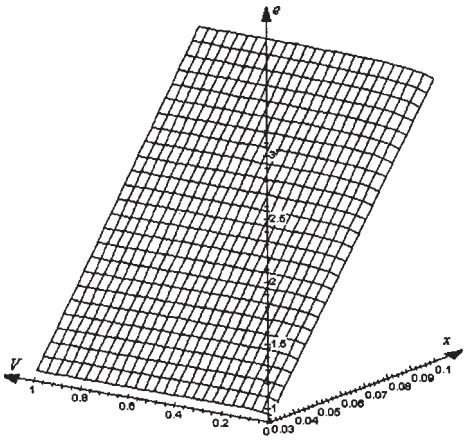

Fig. 4 Graphical representation of *e=e(V, x)*

The graphical representation of *e* (for a volumetric proportion V=0.5) according to the ratio of the elasticity modulus $x=E_2/E$ and the ratio of the fracture limits $y=\sigma_{r1}/\sigma_{1r2}$ is given in figure 5.

The graphical representation of *e* (for a volumetric proportion V=0.5) according to the ratio of the elasticity modulus $x=E_2/E_1$, and the variable $y=E_2\sigma_{r1}/E_1\sigma_{r2}$, for $y>1$, is given in figure 6.

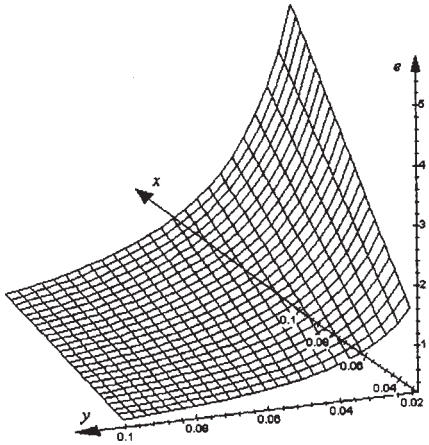

Fig. 5 Graphical representation of *e=e(x, y)*, V=0.5

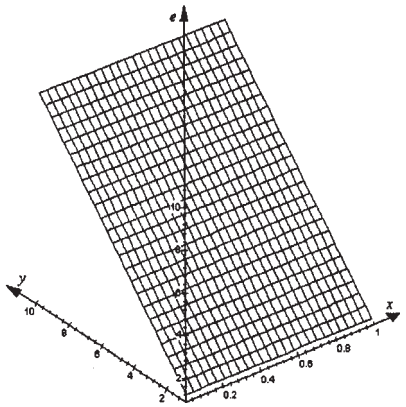

Fig. 6 Graphical representation of *e=e(x, y)*, y>1

The graphical representation of e (for a volumetric proportion V=0.5) according to the ratio of the elasticity modulus $x=E_2/E_1$ and variable $y=E_2\sigma_{r1}/E_1\sigma_{r2}$,, for $y<1$, is given in figure 7.

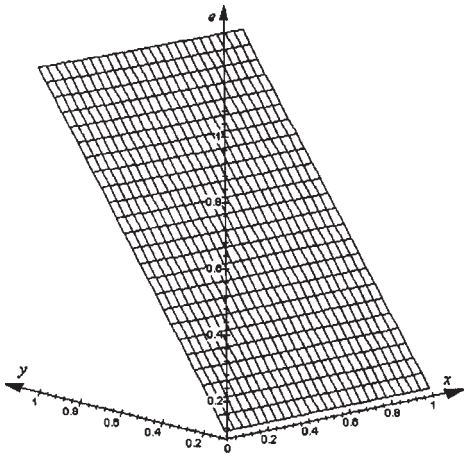

Fig. 7 Graphical representation of *e=e(x, y), y<1*

The graphical representation of *e* according to the volumetric proportion *V* and the ratio of the elasticity modulus $x=E_2/E_1$, in the case in which the ratio $E_2\sigma_{r1}/E_1\sigma_{r2}$, is equal with 1, is given in figure 8.

Experimental determinations and discussions

We made plates from polyesteric resin reinforced with: fiber glass fabrics, carbon fiber fabrics and carbon-kevlar fiber fabrics. From these plates, we made test samples, which have the reinforcement orientated on two perpendicular directions (these coincide with the orthotropic directions of plates). In figures 9 and 10 are presented the test samples which are reinforced with fiber

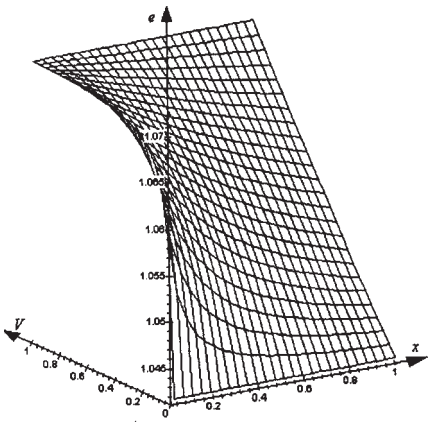

Fig. 8 Graphical representation of $e=e(V, x), y = 1$

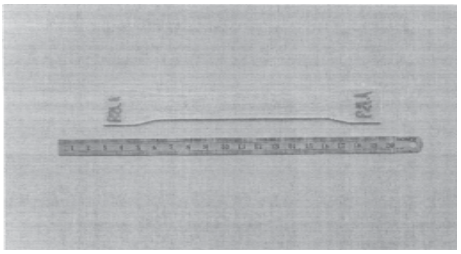

Fig. 9 Sample reinforced with fiber glass

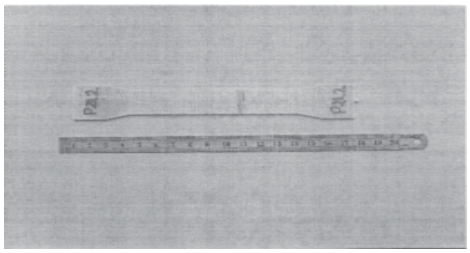

Fig. 10 Sample reinforced with fiber glass

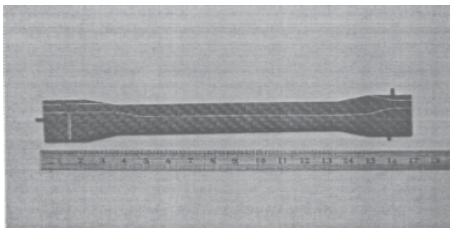

Fig.11 Sample reinforced with carbon fibres

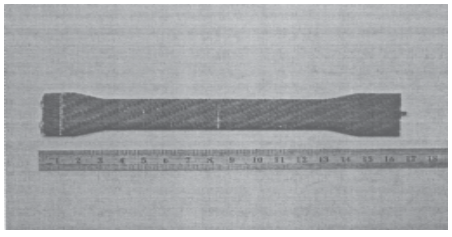

Fig.12 Sample reinforced with carbon fibres

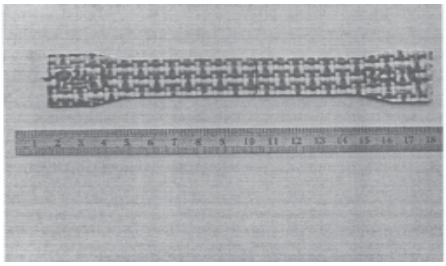

Fig.13 Sample reinforced with carbon- kevlar fibres

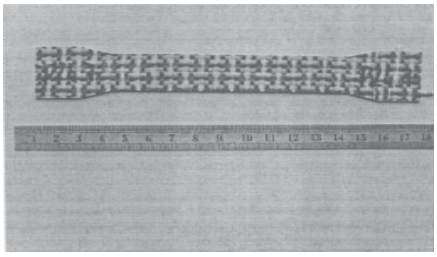

Fig.14 Sample reinforced with carbon-kevlar fibres

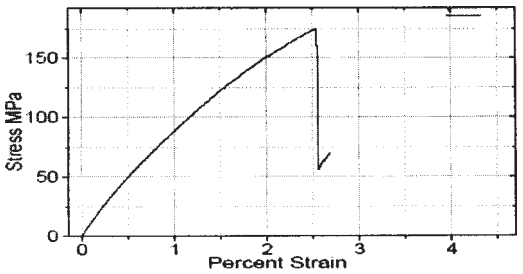

Fig.15. Characteristic curves for test samples reinforced with woven of fibers glass

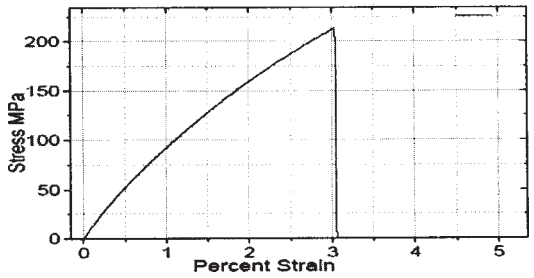

Fig. 16. Characteristic curves for test samples reinforced with woven of fibers glass

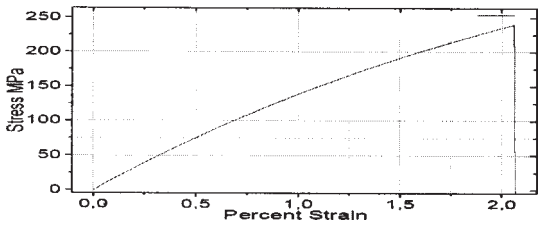

Fig.17. Characteristic curves for test samples reinforced with woven of carbon fibres

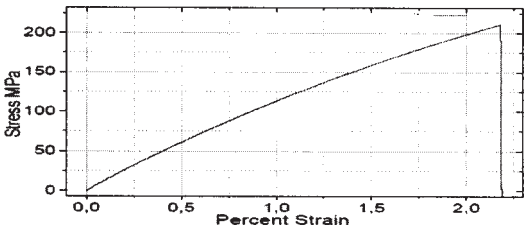

Fig.18. Characteristic curves for test samples reinforced with woven of carbon fibres

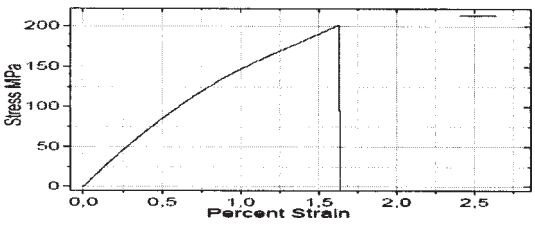

Fig.19. Characteristic curves for test samples reinforced with woven of carbon- kevlar fibres

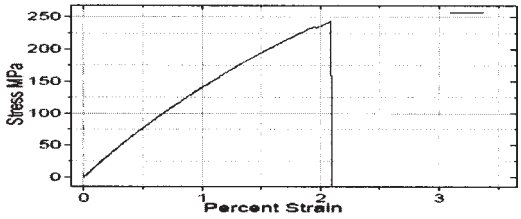

Fig.20. Characteristic curves for test samples reinforced with woven of carbon-kevlar fibers

Type of fabrics	Direction	Elasticity Modulus $[MPa]$	$\sigma_{fracture}$ $[MPa]$	$\sigma_{0,2}$ $[MPa]$	$\varepsilon_{fracture}$ %
Fiber glass	x	10440	175,3	92,26	2,61
	y	11940	213,6	98,61	3.06
Carbon Fibers	x	25090	240,2	164	2,01
	y	23540	211,1	139,5	2,18
Carbon- Kevlar Fibers	x	16550	202,1	145,7	1,64
	y	18870	243,1	164,6	2,09

Table 1

Type of fabrics	Direction	The theoretical elasticity modululs $[MPa]$		The experimental elasticity modulus $[MPa]$
		Calculated with (14)	Calculated with (15)	
Fiber glass	x	9616	9480	9840
	y	10832	10650	10940
Carbon Fibers	x	22899	22758	23090
	y	20640	20498	20540
Carbon-Kevlar Fibers	x	16072	16012	16550
	y	18568	18508	18870

Table 2

glass, in figures 11 and 12 are presented the test samples which are reinforced with carbon fibers, and in figures 13 and 14 are presented the test samples which are reinforced with carbon-kevlar fibers.

All sets of test samples were subject to traction. In figures 15 and 16 are presented the characteristic curves for test samples reinforced with fiber glass fabrics.

In figures 17 and 18 are presented the characteristic curves for test samples reinforced with carbon fiber fabrics.

In figures 19 and 20 are presented the characteristic curves for test samples reinforced with carbon-kevlar fiber fabrics.

In table 1 are given the numerical values of the experimental measurements, for those six types of samples (like average for three samples which have the highest fracture limit).

In table 2 are given, comparatively, the values of the elasticity modules calculated theoretically with (14) and (15) and the values measured experimentally.

It is noted that (14), in which we take into account the Poisson ratios, gives for the longitudinal modulus, values close to those experimentally determined. Differences in the longitudinal modulus of elasticity values calculated with relations (14) and (15) are obvious if the Poisson ratios for the two materials of the beam are very different and are negligible when the Poisson ratios have close values.

It is noted that the variation of the longitudinal modulus of elasticity, when we take into account the Poisson ratios, is nearly proportional with the volumetric proportion of reinforcement. Thus, in practical applications, especially when the Poisson ratios for the fiber and matrix are close, we can use (15) (which is much easy to use, from mathematical point of view) for calculating the longitudinal modulus of elasticity.

Analysis of the graphics which give the variation of parameter e, shows that for the test samples made from epoxy resin reinforced with glass, carbon and carbon-kevlar, this parameter has generally supra-unitary values, which shows that the fracture of the test sample occurs when the fabrics is fractured. This shows that in the case of a tensile test, the resistance of the test sample is given by the fibers and not by the matrix. It is possible, that for a very small volumetric proportion of the reinforcement, the parameter to be subunitar, so the tensile strength is provided by the matrix.

References

1. HARSIN, Z., ROSEN, B.M., Fibers Composites Analysis and Design, vol. I, Composite Materials and Laminates, Material Science Corporation, 1983.
2. YANG, P.C., NORRIS, C.H., STAVSKY, Y., Elastic Wave Propagation in Heterogeneous Plates, Int. Jour. Solids. Struct., **2**, 1965, p. 664-684.
3. WHITNEY, J.M., PAGANA, N.Y., Shear Deformation in Heterogeneous Anisotropic Plates, Jour. Appl. Mech., **37**, 1970, p. 1031
4. REDDY, J.N., A Review of Refined Theories of Laminated Composites Plates, Shock and Vibration, **22**, 1990, p. 3-
5. LIBRESCU, L., Formulation of an Elastodynamic Theory of Laminated Shear Deformable Flat Panels, Journ. Sound and Vibr., **147** (2), 1989, p. 1
6. LIBRESCU, L., KHDEIR, A.A., Analysis of Symmetric Crass-Ply Laminated Elastic Plates Using a High-Order Theory, Part. I: State of Stress and Displacement, Composites Structures, **79**, 1990, p. 189
7. CIUCĂ, I., BOLCU, D., STĂNESCU, M.M., MARIN, GH., Mat. Plast., **45**, no. 3, 2008, p. 279
8. MEAD, D.J., A comparison of some equation for the flexural vibration of damped sandwich beam, Jour. Sound and Vibration, **83**, 1982, p. 363
9. DI TARANTO, R.A., Theory of vibratory bending for elastic and visco-elastic layered finite length beams, ASME Jour. Appl. Mech., **32**, 1965, p. 881
10. MEAD, D.J., MARKUS, S., The forced vibration of three layers, damped sandwich beam with arbitrary boundary condition, Jour. Sound and Vibration, **10**, 1969, p. 163
11. XAVIER, B.P., CHEW, C.H., LEE, K.H., An improved zig-zag model for the vibration of soft cared unysimmetric sandwich beams, Compas. Engineering, Vol. 4, no. 5, 1994, p. 549

12.LADEVEZE, P., Sur une theorie de l'endommagement anisotrope, Rapport Interne No. 34, Laboratoire de Mecanique et Technologie, Cachan, France, 1983
13.LADEVEZE, P., Sur la mecanique de l'endommagement des composites, Compte-Rendus des JNC 5, Pluralis, Paris, 1986, p. 667
14. LEMAITRE, J., CHABOCHE, J.L., A nonlinear model of creep-fatigue damage cumulation and interaction, Proc. IUTAM Symp. On Mechanics of Visco-elastic Media and Bodies, Springer, Gothenburg, 1974
15. HERAKOVICH, C., Mechanics of fibrous composites, John Wiley & Sons, New York, 1998
16.HIEL, C.C., SUMICH, M., CHAPPELL, D.P., A curved beam test specimen for determining the interlaminar tensile strength of a laminated composite, Journal of Composite Materials, **25**, 1991, p. 854
17.GU, Q., REDDY, J.N., Non-linear analysis of free-edge effects in composite laminates subjected to axial loads, International Journal of Non-Linear Mechanics, **276**, 1992, p. 27
18.ZGÎRIAN, G., DEMETRESCU, I., GHEORGHIU, H., IOVU, H., HADAR, A., ATANASIU, C., Rev. Chim. (Bucharest), **56**, no. 7, 2005, p. 757
19.HADAR, A., NICA, M.N., CONSTANTINESCU, I.N., PASTRAMA, ST., The Constructive and Geometric Optimization of the Junctions in the Structures Made from Laminated Composite Materials, STROJINSKI VESTNIK – JOURNAL OF MECHANICAL ENGINEERING, **52**, no. 7-8, Jul-Aug. 2006, p. 546
20.DAVILA, C.G., JOHNSON, E.R., Analysis of delamination initiation in postbuckled dropped-ply laminates, AIAA Journal, 31(4), 1993, p. 721
21.HILTON, H.H., YI, S., Stochastic viscoelastic delamination onset failure analysis of composite, Journal of Composite Materials, **27**(11), 1993, p. 1097

Manuscript received: 16.05.2011